Human Molecular Genetics, 2014 **1–11**
doi:10.1093/hmg/ddu393

Functional screening in *Drosophila* reveals the conserved role of REEP1 in promoting stress resistance and preventing the formation of Tau aggregates

Chiara Appocher, Raffaella Klima and Fabian Feiguin*

International Centre for Genetic Engineering and Biotechnology, Padriciano 99, Trieste 34149, Italy

Received June 3, 2014; Revised and Accepted July 27, 2014

Pathological modifications in the microtubule-associated protein Tau is a common characteristic observed in different neurological diseases, suggesting that analogous metabolic pathways might be similarly affected during neurodegeneration. To identify these molecules and mechanisms, we utilized *Drosophila* models of human Tau-mediated neurodegeneration to perform an RNA interference functional screening against genes considered to be implicated in the pathogenesis of different neurodegenerative disorders. We found that the downregulation of the *Drosophila* REEP1 homolog protein enhanced Tau toxicity with increased formation of insoluble aggregates. On the contrary, the overexpression of either the *Drosophila* or the human REEP1 protein was able to revert these phenotypes and promote neuronal resistance to ER stress. These studies identify a new function for the REEP1 protein *in vivo* and a novel cellular mechanism to prevent Tau toxicity.

INTRODUCTION

The neurodegenerative diseases include a large number of heterogeneous disorders typically characterized by pathological accumulation of abnormally folded proteins, inside the nucleus or in the cytoplasm. These inclusions affect neuronal survival and promote the appearance of progressive neurological symptoms that comprise loss of memory, alterations in intellectual capabilities and/or defects in motor control (1–3).

Regarding to that, the presence of neurofibrillary tangles of the hyperphosphorylated microtubule-binding protein Tau represents one of the most common histological modification observed in postmortem brain tissues of patients affected from different neurological diseases (4,5). For instance, besides Alzheimer's disease, defects in the metabolism of the Tau protein were described in neurological syndromes such as Parkinson's disease (6), Huntington's disease (7), Pick's diseases (8,9), ataxias (10), metabolic alterations in axonal homeostasis like hereditary spastic paraplegias (HSP) (11,12) and systemic forms of encephalopathy (13,14) including progressive modes of Leukoencephalopathy (15,16) and some lipid storage disorders as Niemann–Pick C's disease (17). These reports strongly suggest that similar metabolic pathways, related with the Tau metabolism, might be commonly altered in these pathological conditions. In order to identify these molecules and the mechanisms by them regulated, we utilized the well-established *Drosophila melanogaster* model to perform a functional genetic screening *in vivo*. For these experiments, we expressed the wild-type human Tau full-length isoform (2N/4R) in the fly retina to induce a sensitive, neurodegenerative, background and searched for potential modifiers of this phenotype among a number of genes previously described to be implicated in the pathogenesis of the various neurological diseases described above (18). Interestingly, we found that the strongest modifier of Tau-dependent neurodegeneration in our screening corresponded to the *Drosophila* gene CG42678, the homolog of the human receptor expression enhancing protein (REEP1), primarily associated with the HSP disorder (19–24). For this reason, in the present study, we decided to investigate the function of *Drosophila* CG42678 *in vivo* and define its role in the mechanisms behind Tau-mediated neurodegeneration.

RESULTS

To identify new regulators of Tau toxicity *in vivo*, we performed a bibliographic selection of genes considered to be directly

*To whom correspondence should be addressed at: International Centre for Genetic Engineering and Biotechnology (ICGEB), Padriciano 99, 34149 Trieste, Italy. Tel: +39 0403757201; Fax: +39 040226555; Email: fabian.feiguin@icgeb.org; feiguin@icgeb.org

involved in the pathogenesis of unrelated neurodegenerative diseases which commonly present pathological alterations in the metabolism of the microtubule-binding protein Tau (18). From the total list of candidate genes, 35 of them presented homolog counterparts in *Drosophila melanogaster* to continue with this analysis (Supplementary Material, Table S1).

To determine which of these genes presented the capacity to modulate Tau toxicity *in vivo*, we performed a systematic gene suppression screening by crossing Tau-expressing flies with a collection of transgenic flies carrying an RNA interference (RNAi) sequences against the candidate genes (25,26) (see also Supplementary Material, Table S2). For these experiments, 65 independent RNAi lines (more than one per gene) were crossed against GMR-Gal4 flies expressing human Tau in their retinas (GMR-Gal4, UAS Tau) and the gene Dicer-2 to potentiate the silencing efficiency (26) (Table 1). In addition, to test the specificity of these genetic interactions, the RNAi lines were similarly expressed in the nervous system (using Elav-Gal4) without Tau in the genetic background and the potential neurological phenotypes evaluated in motility assays (see Table 1). We observed that the majority of the silenced genes enhanced the neurodegeneration induced by Tau expression (16 genes), while only four genes acted as genetic suppressors of the phenotypes induced by Tau expression (Table 1). In particular, we found that the genetic interactions with the RNAis against the coding gene CG42678 (ID number 39473 and 39474) strongly enhanced the neurotoxic effects induced by Tau expression, as reflected by the increased reduction and disorganization of the eye surface detected in these insects (Supplementary Material, Fig. S1G and H). Interestingly, we saw that the expression of the CG42678-RNAis alone did not produce apparent defects in these retinas (Supplementary Material, Fig. S1C and D), indicating that this gene may exert a protective role against the neuronal degeneration induced by Tau.

Table 1. Summary of the functional genetic screening

Human gene	Fly gene	Phenotypic effect of modifiers	
		Effect on EYE (UAS Tau present)	Effect on CNS (UAS Tau absent)
		Enhancers	
ACAT1	CG10932	++++	/
BACE2	CathD	++++	/
CDK11/PITSLRE	PitsIre	++++	/
GSK-3B	Sgg	++++	/
HMGCR	Hmgcr	++++	/
REEP1	CG42678	++++	/
CDK5	Cdk5	+++	/
BLMH	CG1440	+++	/
CASP6	Ice	+++	/
CHRNA6	NAcRa96Aa	++	/
MLF2	Mlf	++	/
MRPL46	MRpL46	++	/
PPID	Cyp1	++	/
PPM1J	CG17598	++	/
PSAP	Sap-r	++	/
UBQLN1	Ubqn	++	/
NDUFA8	CG3683	+	***
NDUFB8	CG3192	+	***
CCNT-1	CycT	+++	Let
		Suppressors	
IDE	Ide	− −	/
LRPAP1	CG8507	− −	/
STK38	Trc	− −	/
LIPA	Mag	−	/
		Lethal	Lethal
ACTG1	Act79B	Let	Let
KIF11	Klp61F	Let	Let
KLC4	Klc	Let	Let
		No effect on EYE	No effect on CNS
ALDH1A1	Aldh	/	/
ALDH18A1	Atf-2	/	/
ATF2	Atf2	/	/
EDF1	Mbf-1	/	/
MRPL37	MRpL37	/	/
NDST2	Sfl	/	/
SCP2	ScpX	/	/
SERPINI1	Spn1	/	/
SLC25A17	CG32250	/	/

Results obtained after the RNAi silencing of 35 genes in fly eyes expressing human Tau (GMR-Gal4 driver) and in central nervous system without Tau expression in the genetic background (CNS, with Elav-Gal4). The phenotypic interaction of the modifiers was indicated as enhancer or suppressor of the Tau phenotype. The entity of enhancement was reported as follow: very severe rough (++++), moderate rough (+++), mild rough (++) and very mild rough (+). The entity of suppression was indicated as mild suppression (− −) and very mild suppression (−). The lethal modifiers were indicated as (LET). The neurological defects in Tau-free backgrounds were indicated as asterisks. The bar indicated that no phenotype was revealed upon silencing.

Molecular characterization of *Drosophila* REEP1 function *in vivo*

The Drosophila CG42678 gene belongs to the REEP/DP1/Yop1p family, a group of evolutionary very well-conserved proteins from plants to mammals (Fig. 1A). A bioinformatic analysis indicated that the sequence CG42678 presented strong homology with the human protein REEP1 (33.7% identity and 9.4% similarity) (20,24,21). The level of amino acids conservation among these proteins is particularly higher in their N-terminal region, where they present two hairpin-like hydrophobic regions and share a 66.2% of homology (Supplementary Material, Fig. S2A). In relation with this analysis, we decided to name this gene as *Drosophila* reep1 (D-reep1).

The D-reep1 locus is predicted to encode 13 transcripts (www.Flybase.org), therefore, to determine the expression levels and the anatomical distribution of D-reep1 transcripts (Fig. 1B), we performed a northern blot analysis of poly (A) mRNAs isolated from heads and bodies of 1-day-old adult flies (Fig. 1C). Five different probes where PCR amplified and used for the northern blot analysis (P1–5, Fig. 1B). These experiments confirmed the presence of different transcripts that diverge in their molecular weight, in agreement with the ESTs annotation present in Flybase. We observed a high-molecular-weight band, lightly <3.0 kb, compatible with the isoforms RI, RJ, RH, RQ, RP and RG. An intermediate band of ∼2.0 kb may correspond to the transcripts RK, RR and RS. A lower molecular-weight band of ∼1.5 kb was compatible with the isoforms RD and RE, as reported in Supplementary Material, Table S3. This analysis, nevertheless, helped to confirm the presence of the isoforms RG, RD and RE, specifically recognized by the probe P3 (Fig. 1C, P3). The identity of these transcripts was confirmed by the sequencing of these products and the sequences were submitted to Genbank.

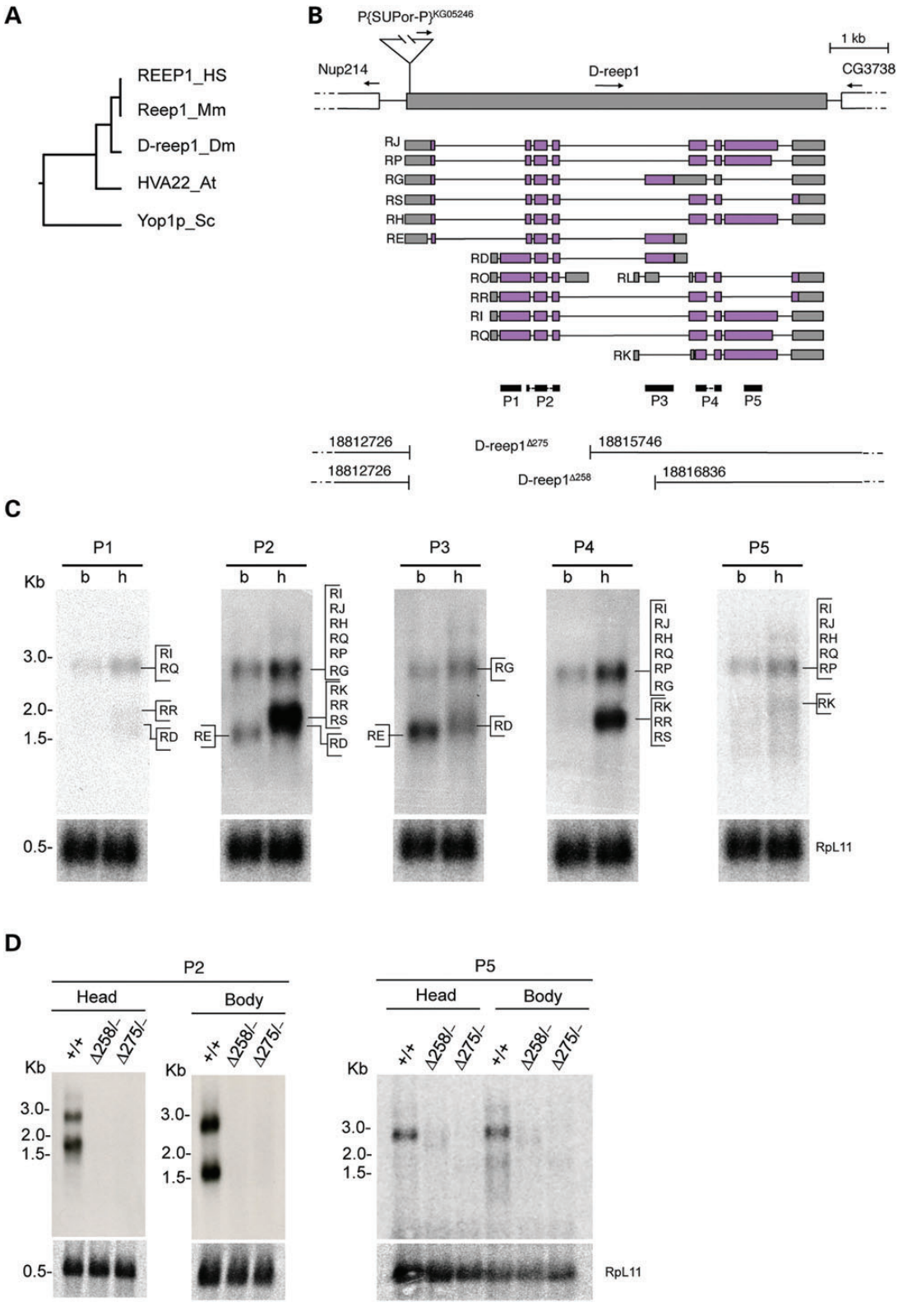

Figure 1. Molecular characterization of the D-reep1 genomic locus. (**A**) Rooted phylogenetic tree of REEP proteins generated by multiple sequence alignment ClustalW in GenomeNet showed the strong conservation among *Homo sapiens* (Hs), *Mus musculus* (Mm), *Drosophila melanogaster* (Dm), *Arabidopsis thaliana* (At) and *Saccaromyces cerevisiae* (Sc). (**B**). Genomic map of the D-reep1 locus with the insertion site of the P-element P[SupOR-P]^{KG05246} and the 13 alternative transcripts predicted (RJ-RK). P1, P2, P3, P4 and P5 indicated the probes utilized in the northern blot analysis. Broken lines at the bottom indicated the extension of the genomic deletions generated for D-reep1$^{\Delta 275/-}$ and D-reep1$^{\Delta 258/-}$, loss-of-function alleles. Scale bar: 1 kb. (**C**) Northern blot analysis of polyadenylated mRNA isolated from heads (h) and bodies (b) of wild-type flies (w^{1118}). RpL11 was used as internal control. (**D**) Northern blot analysis of wild-type, D-reep1$^{\Delta 275/-}$ and D-reep1$^{\Delta 258/-}$ null alleles probed with P2 and P5.

To analyze the function of this gene *in vivo*, we utilized the P-element KG05246 located in the 5′UTR region of D-reep1 to generate chromosomal deletions in this genomic region (Fig. 1B). With this approach, we managed to generate two excised alleles, D-reep1$^{\Delta 258}$ and D-reep1$^{\Delta 275}$, which presented 4.1 and 3.0 kb genomic deletions, respectively, that completely removed the endogenous transcripts of D-reep1 as confirmed by the northern blot analysis performed on 1-day-old flies, hybridized with the probes P2 and P5 that recognize a common region in D-reep1 shared by all the predicted transcripts (see above and Fig. 1D). The data, therefore, indicates that D-reep1$^{\Delta 258}$ and D-reep1$^{\Delta 275}$ flies can be considered as null alleles of the D-reep1 locus.

Phenotypic analysis of homozygous D-reep1$^{\Delta 258}$ and D-reep1$^{\Delta 275}$ alleles indicated that these flies were perfectly viable after embryogenesis and did not present developmental delays during larval grow or pupa formation. In addition, we noticed that D-reep1 mutant flies were perfectly viable, fertile and no modifications in their lifespan were detected compared to controls. Genetic combinations between the D-reep1 alleles and the genomic deficiency Df(2R)BSC784 in the D-reep1 locus did not modify the results described above (Supplementary Material, Fig. S2C). Similarly, heteroallelic combinations between these alleles did not revealed neurological alterations in locomotive behaviours (evaluated in climbing assays) during *Drosophila* aging (Supplementary Material, Fig. S2B), in disagreement with previous data regarding the lack of REEP1 function in mice (27).

D-reep1 co-localizes with ER membrane markers in *Drosophila*

To better characterize the function of D-reep1, we raised polyclonal antibodies against the amino acid stretch 85-STLYRKFVHPML-96 and utilized this probe to determine the intracellular localization of the protein by immunocytochemistry. The staining of third instar larval brains revealed that D-reep1 was present in the tubule-vesicular structures that distributed around the nucleus of elav-positive neurons (Fig. 2A, arrowheads). More importantly, we observed that this labelling was absent in D-reep1 null alleles confirming the specificity of the antibody staining and the particular distribution of the protein (Fig. 2B). To establish the identity of the organelles labelled by the antibody, we stained the body muscles of *Drosophila* third instar larvae. Compared with neurons, these cells present a more extended cytoplasm and, accordingly, we found that D-reep1 presented a similar tubule-vesicular distribution along the very well-organized structures that spread from the nuclear area to the complete intracellular surface (Fig. 2C and D). This cytoplasmic localization of D-reep1, strongly resembled the intracellular distribution of the endoplasmic reticulum (ER) and, to confirm this hypothesis, we expressed the ER luminal protein KDEL-tagged GFP (24B-Gal4/UAS-GFP-KDEL) in third instar larvae muscles

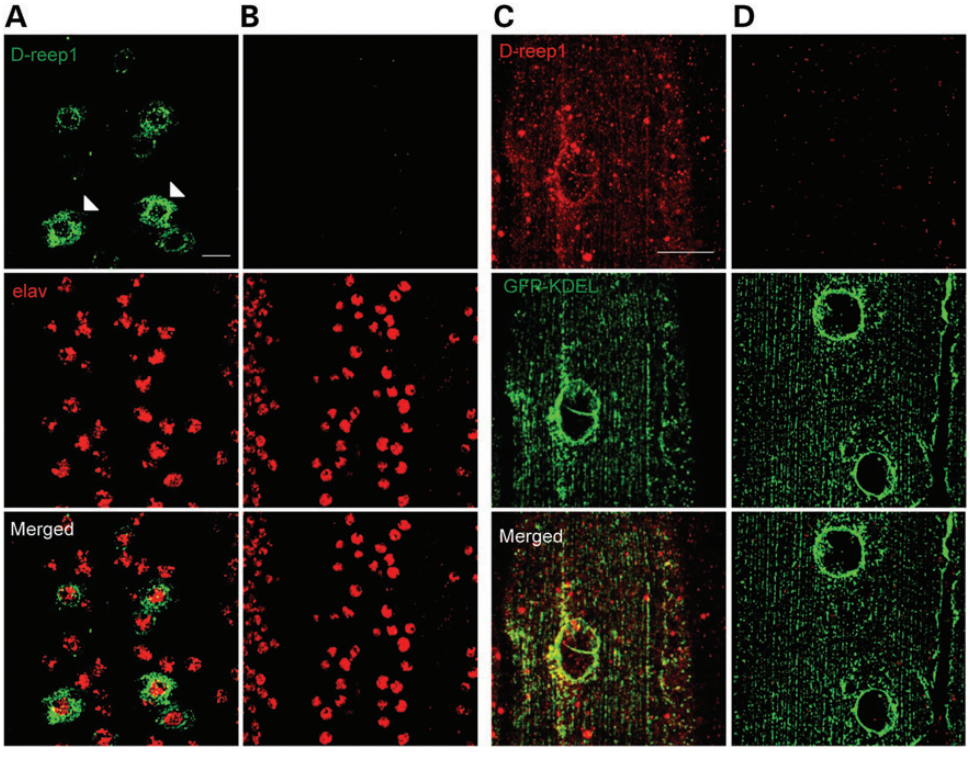

Figure 2. D-reep1 localizes in ER compartment. (**A** and **B**) Confocal images of *Drosophila* third instar larval brains stained with anti-D-reep1 (green) and anti-elav (red) antibodies. (A) Wild-type (w^{1118}). The white arrows indicated the distribution of D-reep1 inside tubular–vesicular structures around the nucleus of dorsal motoneurons. (B) D-reep1$^{\Delta 275/\Delta 258}$. D-reep1 protein was absent in transheterozygote null neurons demonstrating the specificity of this staining. Scale bar: 10 μm. (**C** and **D**) Confocal images of *Drosophila* third instar larval muscles expressing the ER marker, UAS-GFP-KDEL, stained with anti-GFP (green) and anti-D-reep1 (red) antibodies. (C) Muscles of 24B-Gal4/UAS-GFP-KDEL control larvae. The GFP antibody stained the typical tubular network of the ER and perfectly overlaps with D-reep1 (C, merged). (D) Muscles of D-reep1$^{\Delta 275/\Delta 258}$; 24B-Gal4/UAS-GFP-KDEL larvae. Second panel showed that the organization of the ER is not affected in D-reep1 null alleles. Scale bars: 20 μm.

to perform similar co-staining experiments utilizing antibodies against D-reep1 and GFP. The analysis showed a perfect overlap between these antigens throughout the complex organization of the tubular membranes that comprise the ER in larval muscles, confirming the conserved intracellular localization of D-reep1 inside this organelle *in vivo* (Fig. 2C), as previously reported that describing the ER distribution of the mammalian protein REEP1 (22,27,28).

Interestingly, the ER staining performed in larval muscles also highlighted that the formation and elongation of the GFP-KDEL-positive tubule-vesicular structures were not macroscopically affected by the absence of D-reep1 (Fig. 2D). In agreement with this idea, we observed that genetic combinations between the different D-reep1 loss-of-function alleles did not showed differences in the distribution of GFP-KDEL-positive tubule-vesicular membranes or in the subcellular area occupied by the ER, compared with controls (Fig. 2C), suggesting that D-reep1 is not required for the intracellular assembly, transport and distribution of the ER in larval muscles.

D-reep1 function is required for the neuronal response to ER stress

Although the morphological studies described above indicated that D-reep1 seemed not to be involved in the structural organization of the ER, the intracellular localization of the protein still allowed us to hypothesize that D-reep1 might be required to perform metabolic functions inside the ER. Regarding to these issues, an important function of this organelle is to confer resistance against the cellular stress produced by the presence of abnormally folded proteins in the cytoplasm (29,30) and, more specifically, the neurodegeneration provoked by the formation of insoluble Tau aggregates (31,32). To analyze these possibilities, we tested if the lack of D-reep1 affected the physiological response of adult flies to cellular stress *in vivo* by measuring the resistance of these insects to heat-shock stress (see Materials and Methods) (33–35). For these assays, we placed wild-type and D-reep1 mutant flies at 39°C in a water bath and measured the time required to knock down these flies. Thus, we observed that homozygous D-reep1 mutants alone or in allelic combinations with the genomic deficiency in the locus, showed a lower resistance to high temperatures compared with control flies w^{1118} (Fig. 3A, see left panel), suggesting that D-reep1 was required to provide resistance against the cellular stress produced by high temperatures in adult flies. To investigate the specificity of these results, we decided to rescue D-reep1 minus phenotypes by reintroducing the deleted gene and, moreover, to analyze if the human REEP1 protein was able to replace the function of the endogenous gene *in vivo*. For these experiments, we generated transgenic flies containing flag-tagged forms of D-reep1 and human REEP1 and expressed

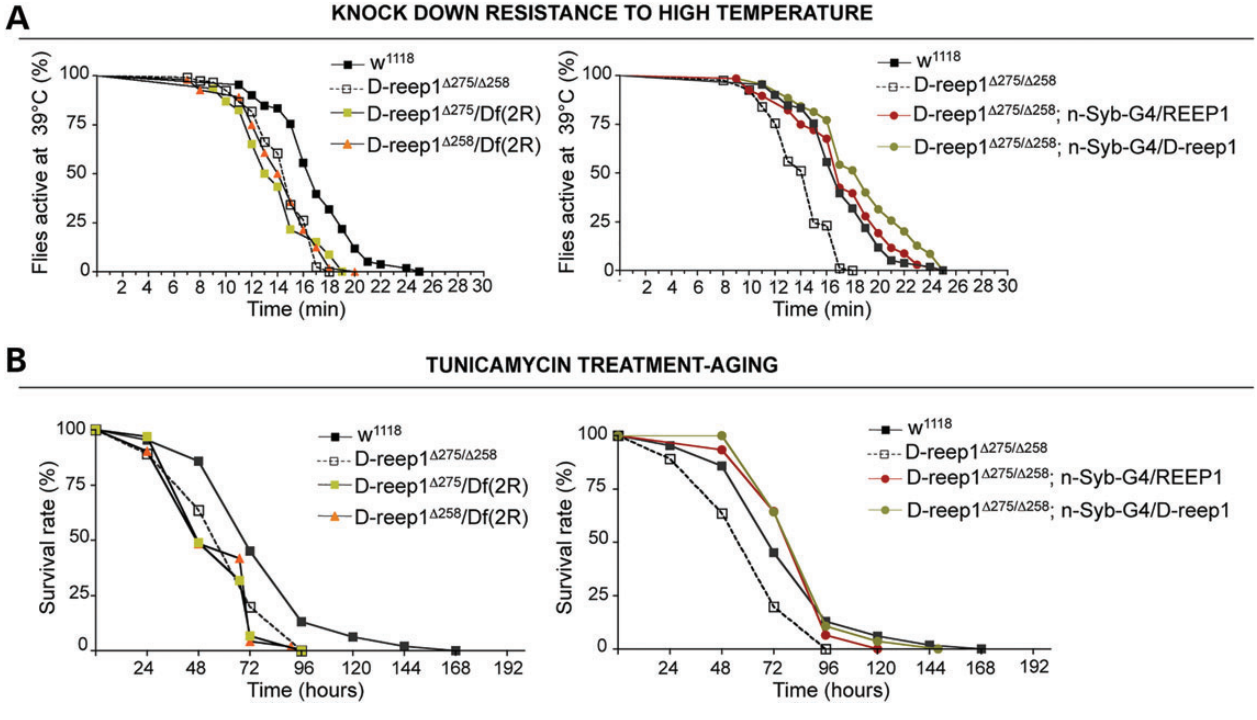

Figure 3. D-reep1 function is required to promote stress resistance. (**A**) The panels show the percentage of flies knocked down in condition of heat stress at 39°C. Left panel: the transheterozygote D-reep1$^{\Delta 258/\Delta 275}$ and each mutant allele in combination with the deficiency of the locus (D-reep1$^{\Delta 258}$/Df(2R)BSC784 and D-reep1$^{\Delta 275}$/Df(2R)BSC784) show less resistance to heat stress at 39°C than the control (w^{1118}). $P < 0.001$, one-way ANOVA. Right panel: the heat stress resistance has been restored by the expression of UAS D-reep1 and UAS REEP1 transgenes with nSyb-Gal4 driver in null D-reep1 background. $P < 0.001$, one-way ANOVA. (**B**) Left panel: survival time course to tunicamycin treatment showed that the median lifespan in D-reep1 minus genetic background was reduced. Median lifespans were (left panel) 72 h for w^{1118} ($n = 243$), 55 h for D-reep1$^{\Delta 258/\Delta 275}$ ($n = 250$), 48 h for D-reep1$^{\Delta 258}$/Df(2R)BSC784 ($n = 170$) and 52 h for D-reep1$^{\Delta 275}$/Df(2R)BSC784 ($n = 170$). Log-rank test and *P*-value: w^{1118} versus D-reep1$^{\Delta 258/\Delta 275}$ ($\chi^2 = 66.60$, $P < 0.0001$), w^{1118} versus D-reep1$^{\Delta 258}$/Df(2R)BSC784 ($\chi^2 = 141.3$, $P < 0.0001$) and w^{1118} versus D-reep$^{\Delta 275}$/Df(2R)BSC784 ($\chi^2 = 123.1$, $P < 0.0001$). Right panel: the expression of UAS D-reep1 or UAS REEP1 with nSyb-Gal4 driver restored the ability to survive to tunicamycin treatment. Median lifespan was (right panel): 96 h for D-reep1$^{\Delta 258/\Delta 275}$; n-Syb-Gal4/D-reep1 ($n = 170$) and D-reep1$^{\Delta 258/\Delta 275}$; n-Syb-Gal4/UAS REEP1 ($n = 170$). Log-rank test and *P*-value: rescue D-reep1$^{\Delta 258/\Delta 275}$; n-Syb-Gal4/UAS D-reep1 versus D-reep1$^{\Delta 258/\Delta 275}$ ($\chi^2 = 54.45$, $P < 0.0001$), D-reep1$^{\Delta 258/\Delta 275}$; n-Syb-Gal4/UAS REEP1 versus D-reep1$^{\Delta 258/\Delta 275}$ ($\chi^2 = 28.44$, $P < 0.0001$).

these proteins in D-reep1 mutant backgrounds in a tissue-specific manner using the GAL4/UAS system. Interestingly, we observed that both D-reep1 and human REEP1 constructs expressed transgenic proteins that localized in the ER of larval muscles *in vivo* (Supplementary Material, Fig. S3A and B). Moreover, we found that the individual expression of the transgenic proteins in postmitotic neurons using the pan-neuronal nSyb-Gal4 driver (36) was able to rescue the resistance of D-reep1 minus flies to heat-shock stress (Fig. 3A see right panel), demonstrating that the function of these proteins is evolutionary conserved and sufficient, inside the ER, to confer stress resistance in heat-shock knockdown assays. To further explore the potential role of D-reep1 in the ER response to cellular stress, we induced a more specific form of intracellular stress *in vivo* by treating wild-type and D-reep1 minus flies with tunicamycin. This drug inhibits the N-glycosylation of membrane proteins inside ER creating the accumulation of misfolded proteins inside the organelle and causing ER stress (37,38) together with the activation of the unfolded protein response (39,40). For these experiments, 1-day-old flies were fed with 12 μM tunicamycin (supplemented in the fly food) and the number of dead flies during the time of exposure to the drug was quantified (34). We found that after 48 h of tunicamycin treatment, wild-type w^{1118} flies presented a mortality rate of ∼12%; on the contrary, this percentage rose up to 40–50% in D-reep1$^{\Delta 258/\Delta 275}$ homozygous null alleles alone or in allelic combinations with the genomic deficiency (D-reep1$^{\Delta 258}$/Df(2R)BSC784 and D-reep1$^{\Delta 275}$/Df(2R)BSC784, see Figure 3B, left panel). Furthermore, we observed that the expression of either D-reep1 or human REEP1 with the neuronal driver nSyb-Gal4 (36) was able to rescue the sensitivity of D-reep1 mutant flies to tunicamycin (Fig. 3B, see right panel), confirming *in vivo* the novel role of this protein in the mechanisms of neuronal resistance against the cellular stress produced by the abnormal protein folding inside the ER.

D-reep1 protects neurons from Tau-mediated degeneration by preventing the accumulation of neurotoxic aggregates

The experiments described before showed that D-reep1 has an important role in promoting neuronal resistance against stressful situations like heat shock or the abnormal accumulation of unfolded proteins in the ER, suggesting that similar defects in stress resistance might be responsible of the increased sensitivity to Tau-mediated neurodegeneration observed in D-reep1 knocked down flies (Supplementary Material, Fig. S1G and H) (31,32). To confirm this hypothesis and understand how alterations in D-reep1 function modifies Tau toxicity, we expressed the human Tau protein in D-reep1 null backgrounds (D-reep1$^{\Delta 258/\Delta 275}$; GMR-Gal4, UAS Tau) and observed that the absence of D-reep1 strongly enhanced the neurodegeneration observed in the *Drosophila* retinas that presented the formation of extensive necrotic areas, visible as black spots, over the eye surface (Fig. 4C and F). Compared with the morphology of Tau-expressing eyes in the wild type, control and backgrounds (GMR-Gal4, UAS Tau/+, Fig. 4B and F), these data confirm the initial results obtained with D-reep1 RNAi expression (Supplementary Material, Fig. S1G and H) and further support the idea that D-reep1 function is required to prevent Tau-mediated neurodegeneration. In order to gain insight into the mechanisms behind the neuroprotective role of D-reep1, we decided to test whether modulations in D-reep1 protein activity were able to modify the formation of insoluble Tau aggregates *in vivo*. To answer these questions, confocal microscope analysis of Thioflavin-S stained third instar larvae eye discs were performed and revealed the presence of amyloid clusters of Tau in control retinas expressing human Tau (GMR-Gal4, UAS Tau/+), (Fig. 4I and M; Supplementary Material, Fig. S4A and E). Besides Tau, these Thioflavin-S-positive clusters co-stained with the filamentous actin marker phalloidin revealing the abnormal formation of actin-rich structures within the amyloid aggregates (41) (see actin staining in Fig. 4I and N; Supplementary Material, Fig. S4A and F). Interestingly, we found that the depletion of D-reep1 strongly increased the pathological formation of Thioflavin-S-positive amyloid aggregates in the mutant retinas as well as the incidence of ectopic actin-rich structures within these amyloid clusters, enhancing the structural defects observed in the organization of these tissues (Fig. 4J and M). On the contrary, increased expression of either D-reep1 or human REEP1 transgenes in Tau-expressing flies (GMR-Gal4,UAS Tau/UAS D-reep1 and GMR-Gal4,UAS Tau/UAS REEP1) strikingly prevented the formation of Thioflavin-S-positive amyloid aggregates of Tau (Fig. 4K, L and M; Supplementary Material, Fig. S4C, D and E) together with the abnormal polymerization of actin filaments inside the amyloid clusters and the general morphology of the eye discs (Fig. 4K, L and N). In adult tissues, the external neurodegeneration induced by Tau expression also appeared strongly ameliorated in D-reep1 or human REEP1 gain-of-function Drosophila eyes (Fig. 4D, E and F). Instead, biochemical experiments performed on the samples described before revealed that differences in D-reep1 or REEP1 activity did not affect the phosphorylation status of Tau *in vivo*. Thus, quantitative western blot analysis of protein extracts obtained from flies expressing Tau in wild-type (GMR-Gal4,UAS Tau) or in D-reep1 modified backgrounds such as (D-reep1$^{\Delta 258/\Delta 275}$; GMR-Gal4,UAS Tau), (GMR-Gal4,UAS Tau/UAS D-reep1) and (GMR-Gal4,UAS Tau/UAS REEP1) did not revealed any differences in the phosphorylation status of the Tau protein for any of the several phospho-specific antibodies utilized AT8, AT180 and Tau1 (42–45) (Fig. 4G). Similarly, the western blots performed and stained with the antibody Tau5 (46) showed that differences in D-reep1 function did not affected the levels of total Tau protein expression *in vivo*, confirming that the activity of D-reep1 is sufficient to protect neurons against Tau-mediated neurodegeneration by, most probably, preventing the abnormal formation or accumulation of Thioflavin-S-positive Tau aggregates.

DISCUSSION

The presence of intracellular aggregates of pathologically phosphorylated Tau in brains of patients suffering from different neurological diseases not described as tauopathies, strongly suggest that defects in Tau homeostasis may represent a common mechanism behind the molecular processes that lead to neurodegeneration. In agreement with this hypothesis, we performed a functional genetic screenings in *Drosophila* through the silencing of several, unrelated, genes previously implicated in the pathogenesis of complex neurodegenerative diseases. Following this approach, we observed that the majority of the suppressed

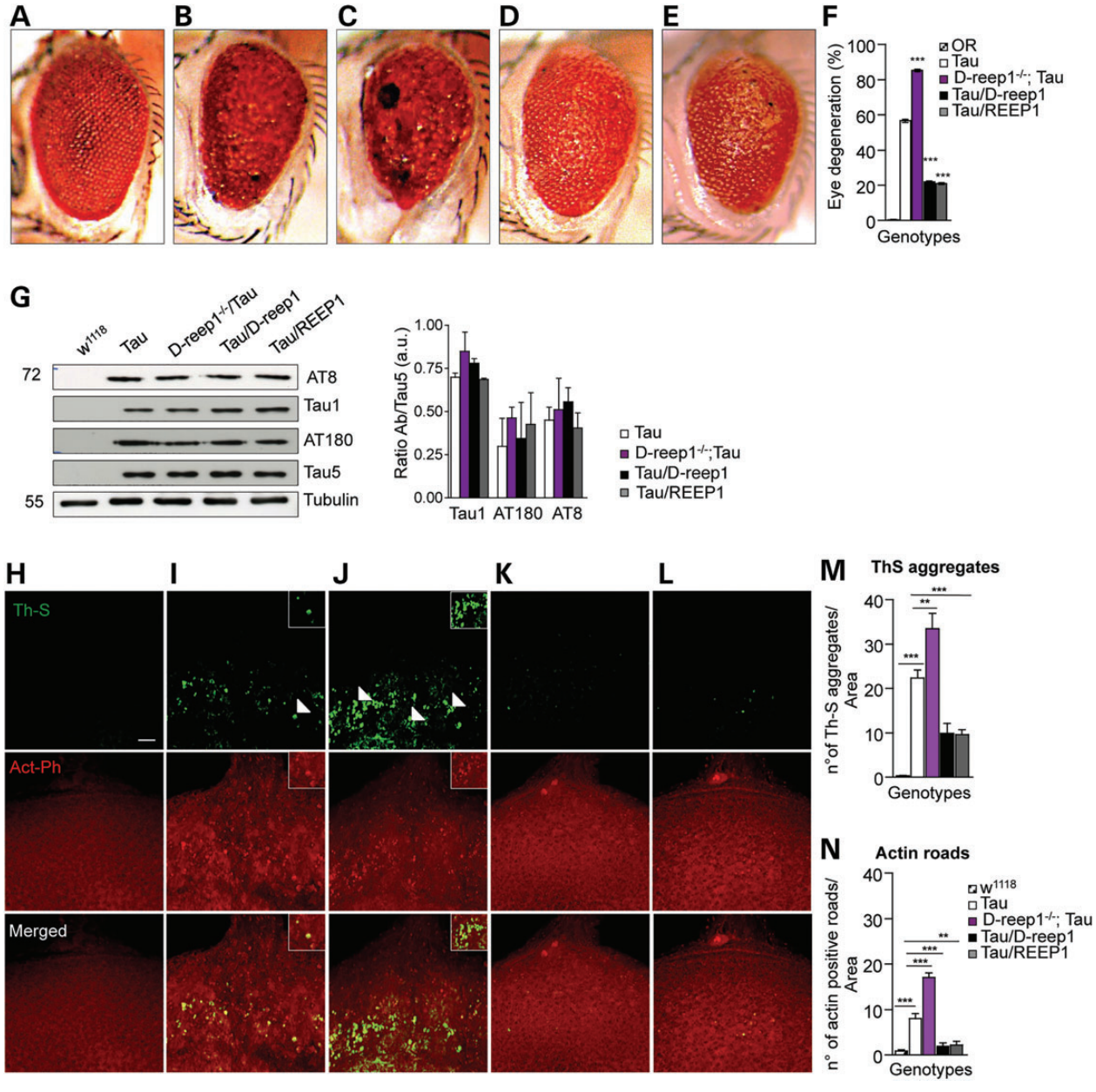

Figure 4. D-reep1 and REEP1 prevent Tau-mediated degeneration and the formation of Thioflavin-S aggregates. Expression of human Tau expression induces an extensive degeneration of in Drosophila eyes in (**B**) GMR-Gal4,UAS Tau/+ flies compared with (**A**) OR, wild-type eye controls. Nevertheless, removing D-reep1 enhanced Tau-induced toxicity in (**C**) D-reep1$^{\Delta 258/\Delta 275}$;GMR-Gal4,UAS Tau/+ flies. On the contrary, the overexpression of D-reep1 (GMR-Gal4, UAS Tau/UAS D-reep1, **D**) or human REEP1 (GMR-Gal4, UAS Tau/UAS REEP, **E**) ameliorated the Tau-induced eye degeneration *in vivo*. (**F**) The graph reports the percentage of the eye surface degenerated. Asterisks indicated significant differences between the genotypes ($n = 50$, $P < 0.001$, one-way ANOVA). (**G**) Western blot analysis indicates that alterations in D-reep1 and/or REEP1 protein levels did not influenced the phosphorylation status of Tau. The genotypes analyzed were respectively w^{1118} (lane 1), GMR-Gal4,UAS Tau/+ (lane 2), D-reep1$^{\Delta 258/\Delta 275}$;GMR-Gal4, UAS Tau/+ (lane 3), GMR-Gal4,UAS Tau/UAS D-reep1 (lane 4) and GMR-Gal4, UAS Tau/UAS REEP1 (lane 5). The total Tau protein was detected with Tau5 antibody. Tau phosphorylation pattern was evaluated with AT8, Tau1 and AT180 phospho-specific antibodies. Tubulin was used as a loading control (bottom panel). The graph on the right represented the quantification of Tau phospholevels by one-way ANOVA, $n = 3$. (**H**–**L**) Confocal images of eye imaginal discs of third instar larvae stained with Thioflavin-S (green) and actin-phalloidin (red). Arrowheads indicated Thioflavin-S-positive and actin deposits in (I) GMR-Gal4, UAS Tau/+ and (J) D-reep1$^{\Delta 258/\Delta 275}$; GMR-Gal4, UAS Tau/+ not presented in the (H) w^{1118} controls. Thioflavin-S aggregates increased in D-reep1 null background (J and **M**) and decreased with the co-expression of UAS D-reep1 and UAS REEP1 (GMR-Gal4, Tau/D-reep1, K and GMR-Gal4,Tau/UAS REEP1, L). Co-localization of actin with Thioflavin-S-positive-structures was shown in the merge. Scale bar: 10 μm. (M) Numbers of Thioflavin-S-positive aggregates per area were presented as average ± SEM ($n = 25$ eye discs). (**N**) Numbers of actin-positive aggregates per area were presented as average ± SEM ($n = 25$ eye discs). Asterisks indicated significant differences between the genotypes ($^{**}P < 0.01$, $^{***}P < 0.001$, one-way ANOVA).

genes enhanced the neurodegeneration induced by human Tau expression in flies (Table 1; Supplementary Material, Table S1) indicating that common pathological mechanisms, shared by different neurological disorders may exist *in vivo*. Alternatively, similar neuroprotective pathways might be comparably activated with counteract Tau toxicity and intracellular stress.

In agreement with this view, we have identified the human homolog protein REEP1 in flies and demonstrate that this is a conserved protein that localizes in the tubule-vesicular membranes of the ER where promotes the intracellular resistance against stressful situations like heat shock or the abnormal accumulation of misfolded proteins in the cytoplasm. In agreement with these results, it was previously reported that HVA22, the plant homolog gene of D-reep1, was required to tolerate stressful situations by inhibiting the activation of programmed cell death in plants growing under adverse conditions (47,48). In *Drosophila*, we found that D-reep1 null alleles did not present evident problems during development or neurological defects associated with aging or alterations in the life span. Similar results were observed in yeast, where null mutations in the D-reep1 homolog gene of YOP1p did not affect cells viability (49). On the contrary, the suppression of REEP1 in mice interfered with the ER structure and reduced the long-term neuronal survival (27), indicating that species-specific differences in the gene function may exist. Regarding to that, we observed that D-reep1 and human REEP1 were identically localized in the ER of *Drosophila* and required to confer stress resistance against the accumulation of unfolded proteins induced by tunicamycin (Fig. 3B). In correlation with these data, we found that D-reep1 function was necessary to prevent Tau-mediated neurodegeneration and aggregates formation (Fig. 4A–E and H–L), suggesting that these results might be connected. Concerning this hypothesis, we found that increased ER stress enhanced the neurodegenerative effect produced by Tau expression *in vivo* (Supplementary Material, Fig. S5A and B). Moreover, we detected that modifications in Tau levels increased the expression amounts of D-reep1 mRNA (Supplementary Material, Fig. S5C), indicating that D-reep1 may form part of the cellular machinery in charged to respond, signal or protect against ER stress *in vivo*.

Regarding the potential mechanisms behind neuronal protection, we found that alterations in D-reep1 or REEP1 function did not affect the total levels of Tau present in *Drosophila* heads suggesting that these proteins might be required to prevent the formation or accumulation of Thioflavin-S-positive Tau clusters rather than promoting the degradation of the aggregates (see Tau5, Fig. 4G). Nevertheless, our data did not discard a potential role of D-reep1 in regulating the removal of the Tau insoluble clusters through ER-dependent autophagy (50,51), further experiments will be necessary to clarify these issues. In summary, this study uncovered a novel and conserved function of the D-reep1 gene in promoting ER stress resistance and preventing Tau-mediated degeneration *in vivo*, most probably by inhibiting the pathological accumulation of Thioflavin-S-positive Tau aggregates. Finally, our data also predict that defects in REEP1 function, in patients with HSP, may lead to alterations in the neuronal responses to ER stress with defects in the metabolism of Tau and general problems in the maintenance of the structural organization and intracellular transport in long axons (52,53).

MATERIALS AND METHODS

Generation of D-reep1 null alleles

The D-reep1 excision lines, alleles D-reep1$^{\Delta 258}$ and D-reep1$^{\Delta 275}$ were generated by imprecise excision of the P{SUPor-P} CG42678^{KG05246} transposon using TfΔ2–3 transposase. The precise excision points were identified by sequencing of PCR amplicons generated with primers flanking P{SUPor-P} CG42678^{KG05246} insertion site.

Generation of UAS D-reep1 and UAS REEP1 flies

Total RNA extracted from fly heads of wild-type flies were retrotranscribed with Superscript III Reverse Transcriptase (#18080044, Life Technologies) in the presence of oligodT and the full-length cDNA of the RG isoform of D-reep1 was amplified. The primers used for amplification of the cDNA were designed on the isoforms RG:

Forward: 5′-ATGATCAGCAGCCTGTTTTCGCG-3′,

Reverse: 5′-TCAGTAGTTTTCCACATCCACATCG-3′.

The human REEP1 cDNA was synthetized from polyA RNA of Caucasian human brain (Clontech#636102). The UAS D-reep1 and the UAS REEP1 cDNAs were FLAG tagged, *Eco*RI–*Xba*I cloned in the pUASTattB and sent to Best Gene, Inc. for the generation of transgenic flies.

Other Drosophila strains

The human full-length Tau cDNA (2N/4R isoform) was a kind gift of Jesus Avila. Tau cDNA was cloned in the pKS69 vector and sent to Best Gene, Inc. for the generation of transgenic flies.

The other strains included: Oregon-R (OR), w^{1118}, UAS mCD8::GFP, UAS Lac-Z and UAS-GFP-KDEL (Bloomington *Drosophila* Stock Center, Bloomington, IN, USA), the pan-neuronal driver nSyb-Gal4 (36), the muscle driver 24B-Gal4 (54) and the eye driver GMR-Gal4 (55). Flies maintenance and crosses were settled on standard cornmeal sucrose and yeast agar medium in a 12 h light–dark cycle at 25°C when not specified.

Eye quantification

External eye phenotypes of 1-day-old CO_2-anesthetized flies were evaluated with a Leica M 205C stereomicroscope and photographed with a Leica DFC420 digital camera. For each genotype, 50 flies were evaluated and quantification of phenotypes was performed splitting ideally the fly's eye in four areas and evaluating the percentage of degeneration in each single sector. All phenotypic evaluations of each analyzed genotype were averaged and compared with genotypes using a control.

Tunicamycin treatment

Survival curves of tunicamycin-treated flies were performed in 12 : 12 hours light–dark cycle at 25°C on a medium composed of 1.3% low-melting agarose, 1% sucrose supplemented with 12 μM tunicamycin (Ascent). Groups of 10 flies, 1 day aged, were transferred in 50 ml tubes containing 1 ml of the medium and once a day until dead flies were scored. For each genotype, a minimum of 140 flies up to a maximum of 250 flies were used.

Heat knockdown sensitivity evaluation to thermal exposure

Group of 10 males, 1 day aged, were transferred in empty vial and immersed in a water bath for 30 min at 39°C. A programmable

heating unit controlled and a proper water circulation ensured controlled temperature. Every minute, knock down flies, sluggish or immobile or upside down were scored. Data from 10 separate experiments were combined to define the curve of thermotolerance for each genotype.

Generation of D-reep1 antibody

A peptide spanning from amino acids 85–96 (STLYRKF VHPMLC) of the PG isoform of D-reep1 was synthetized and used to erase in mouse polyclonal antibody against D-reep1.

Extraction of poly (A) mRNA and Northern blot

For the characterization of the differentially expressed isoforms, 1-day-old adult fly, in batches of 300 females and males, was quickly frozen in liquid nitrogen and vortexed to collect separately heads and bodies. RNA was isolated with TRIZOL (#15596-026 Life Technologies). Poly (A) mRNA was further purified with Dynabeads mRNA purification kit (Life Technologies #61006), and aliquots of 600 ng of poly (A) were resolved on a 1% agarose gel (NorthernMAX kit, #AM1940, Ambion) and transferred to Hybond-N+ membrane (Healthcare #RPN203B). Membranes were UV cross-linked and hybridized with P^{32}-labelled probes (REdiprime DNA labelling system, #RPN1633GE Healthcare) and subsequently acquired by phosphoimager (Cyclone Imaging System). Probes were PCR amplified on cDNAs of D-reep1 gene with the following primers:

P1:for 5′-ATGAGGCCAATCTATCAGCAGGAG-3′
P1:rev 5′-CTCGATCCTCCACTATGTAGGC-3′
P2:for 5′-GGCATATGCCTCATACAAGGCCGTCAG-3′
P2:rev 5′-CTGCATGAGGACATTGGTGGCATAG-3′
P3:for 5′-AACTATGCCACCAATGTCCTC-3′
P3:rev 5′-TCAGTAGTTTTCCACATCCACATCG-3′
P4:for 5′-ATGCATCGCACGCAGGACGAGCTGG-3′
P4:rev 5′-CCACTACTTCTCCGACTTGTTGCGCG-3′
P5:for 5′-CAGTTTGAAGATGCATTGTTTGAGG-3′
P5:rev 5′-GGCCTTGGGCCGCAAGGAGGG-3′

Immunoblot of Drosophila heads

For Tau extraction, flies were frozen in liquid nitrogen, vortexed to collect heads and subsequently squeezed in lysis buffer (150 mM NaCl, 10 mM Tris, 5 mM EDTA, 10% glycerol, 5 mM EGTA, 50 mM NaF, 4 M urea, 5 mM DTT and protease inhibitors) added of 2% SDS, 1× phosphatase inhibitors cocktail 1 and 2 (Sigma) and caliculin A (Calbiochem). Heads protein extracts were sonicated after centrifugation at 8000*g* for 10 min at RT. Proteins quantification was performed with Qbit™ Protein Assay (#Q33211, Life Technologies). Extracted proteins were separated in SDS–PAGE and blotted on 0.2 μm nitrocellulose membrane (Whatman Protran #Z613657). Membranes were blocked in 5% nonfat dried milk in TBS–0.01% Tween 20 and subsequently incubated with primary antibodies properly diluted: anti-Tau5 (1 : 2000, DSHB), anti-Tau1 (1 : 2000, #MAB3420 Chemicon), anti-AT8 (1 : 500, #90206 Autogen Bioclear Innogenetics), anti-AT180 (1 : 1000, #90337 Autogen Bioclear Innogenetics), anti-tubulin (1 : 2000, DM1A #CP06 Calbiochem).

Immunohistochemistry and Thioflavin-S staining

Larval body wall muscles were dissected in saline containing 0.1 mM Ca^{+2}, fixed in ice-cold 4% paraformaldehyde for 20 min, washed in PBS/0.1% Tween 20 and blocked with 5% normal goat serum (NGS; Chemicon #S26-100 ML) for 30 min. Primary antibodies were used for overnight incubation at 4°C: anti-D-reep1 (1 : 20), anti-FLAG M5 (1 : 200, #F4042 Sigma), anti-GFP (1 : 200, #A11122 Life Technologies). Secondary antibodies used: Alexa Fluor® 555 Phalloidin (1 : 150, #A344055 Life Technologies), Alexa Fluor® 488 (mouse #A11001, rabbit #A11008 1 : 500, Life Technologies) Alexa Fluor® 555 (mouse #A21422, rabbit #A21428 1 : 500, Life Technologies).

Dissection of the eye imaginal discs of third instar larvae dissection was performed as previously described (56). The dissected larval brains were permeabilized and incubated overnight in 50% EtOH containing 0.2% Thioflavin-S (#R311820 ThS, Sigma). After washing in 50% EtOH and PBS, brains were stained with Alexa Fluor® 555 Phalloidin in PB/0.3% Triton X-100 5% NGS for 2 h at RT. After incubation larval brains were washed in PBT/0.3% Triton X-100 (3 × 20 min) and left at 4°C for one night in Slowfade®Gold antifade (#S36936, Life Technologies). The day after, the brains were removed and the eye discs were mounted on a glass slide for confocal microscope analysis. Thioflavin-S and actin-positive aggregates were identified by its characteristic stone-like shape and quantified by counting the number of aggregates per tissue areas. More than 25 larval eye discs for each genotype were analyzed.

Statistical analysis

In all experiments, means were compared, as appropriate by one-way ANOVA, with Bonferroni correction for multiple comparisons. The log-rank test was performed to compare the survival of the genotypes analyzed.

SUPPLEMENTARY MATERIAL

Supplementary Material is available at *HMG* online.

ACKNOWLEDGEMENTS

We thank Prof. Jesus Avila (Universidad Autonoma de Madrid, UAM) for Tau4R plasmid, Dr. Corrado Guarnaccia (ICGEB) for peptide synthesis, the Bloomington Stock Center and the Developmental Studies Hybridoma Bank for reagents and others members of the Neurobiology lab for helpful comments and discussions.

Conflict of Interest statement. None declared.

FUNDING

The study was supported by ICGEB intramural fundings.

REFERENCES

1. Shulman, J.M. and De Jager, P.L. (2009) Evidence for a common pathway linking neurodegenerative diseases. *Nat. Genet.*, **41**, 1261–1262.

2. Jucker, M. and Walker, L.C. (2013) Self-propagation of pathogenic protein aggregates in neurodegenerative diseases. *Nature*, **501**, 45–51.
3. Guo, J.L. and Lee, V.M.Y. (2014) Cell-to-cell transmission of pathogenic proteins in neurodegenerative diseases. *Nat. Med.*, **20**, 130–138.
4. Buée, L., Bussière, T., Buée-Scherrer, V., Delacourte, A. and Hof, P.R. (2000) Tau protein isoforms, phosphorylation and role in neurodegenerative disorders. *Brain Res. Brain Res. Rev.*, **33**, 95–130.
5. Kolarova, M., García-Sierra, F., Bartos, A., Ricny, J. and Ripova, D. (2012) Structure and pathology of tau protein in Alzheimer disease. *Int. J. Alzheimers Dis.*, **2012**, 731526.
6. Lei, P., Ayton, S., Finkelstein, D.I., Adlard, P.A., Masters, C.L. and Bush, A.I. (2010) Tau protein: relevance to Parkinson's disease. *Int. J. Biochem. Cell Biol.*, **42**, 1775–1778.
7. Caparros-Lefebvre, D., Kerdraon, O., Devos, D., Dhaenens, C.M., Blum, D., Maurage, C.A., Delacourte, A. and Sablonnière, B. (2009) Association of corticobasal degeneration and Huntington's disease: can Tau aggregates protect Huntingtin toxicity? *Mov. Disord. Off. J. Mov. Disord. Soc.*, **24**, 1089–1090.
8. Delacourte, A., Robitaille, Y., Sergeant, N., Buée, L., Hof, P.R., Wattez, A., Laroche-Cholette, A., Mathieu, J., Chagnon, P. and Gauvreau, D. (1996) Specific pathological Tau protein variants characterize Pick's disease. *J. Neuropathol. Exp. Neurol.*, **55**, 159–168.
9. Arai, T., Ikeda, K., Akiyama, H., Shikamoto, Y., Tsuchiya, K., Yagishita, S., Beach, T., Rogers, J., Schwab, C. and McGeer, P.L. (2001) Distinct isoforms of tau aggregated in neurons and glial cells in brains of patients with Pick's disease, corticobasal degeneration and progressive supranuclear palsy. *Acta Neuropathol. (Berl.)*, **101**, 167–173.
10. Houlden, H., Johnson, J., Gardner-Thorpe, C., Lashley, T., Hernandez, D., Worth, P., Singleton, A.B., Hilton, D.A., Holton, J., Revesz, T. *et al.* (2007) Mutations in TTBK2, encoding a kinase implicated in tau phosphorylation, segregate with spinocerebellar ataxia type 11. *Nat. Genet.*, **39**, 1434–1436.
11. McDermott, C.J., White, K., Bushby, K. and Shaw, P.J. (2000) Hereditary spastic paraparesis: a review of new developments. *J. Neurol. Neurosurg. Psychiatry*, **69**, 150–160.
12. Wharton, S.B., McDermott, C.J., Grierson, A.J., Wood, J.D., Gelsthorpe, C., Ince, P.G. and Shaw, P.J. (2003) The cellular and molecular pathology of the motor system in hereditary spastic paraparesis due to mutation of the spastin gene. *J. Neuropathol. Exp. Neurol.*, **62**, 1166–1177.
13. Tanuma, N., Miyata, R., Kumada, S., Kubota, M., Takanashi, J., Okumura, A., Hamano, S. and Hayashi, M. (2010) The axonal damage marker tau protein in the cerebrospinal fluid is increased in patients with acute encephalopathy with biphasic seizures and late reduced diffusion. *Brain Dev.*, **32**, 435–439.
14. McKee, A.C., Stern, R.A., Nowinski, C.J., Stein, T.D., Alvarez, V.E., Daneshvar, D.H., Lee, H.-S., Wojtowicz, S.M., Hall, G., Baugh, C.M. *et al.* (2013) The spectrum of disease in chronic traumatic encephalopathy. *Brain J. Neurol.*, **136**, 43–64.
15. Powers, J.M., Byrne, N.P., Ito, M., Takao, M., Yankopoulou, D., Spillantini, M.G. and Ghetti, B. (2003) A novel leukoencephalopathy associated with tau deposits primarily in white matter glia. *Acta Neuropathol. (Berl.)*, **106**, 181–187.
16. Brüggemann, N., Gottschalk, S., Körtke, D., Marxsen, J.H. and Moser, A. (2012) Excessively increased CSF tau in progressive multifocal leukoencephalopathy. *Clin. Neurol. Neurosurg.*, **114**, 762–764.
17. Ohm, T.G., Treiber-Held, S., Distl, R., Glöckner, F., Schönheit, B., Tamanai, M. and Meske, V. (2003) Cholesterol and tau protein – findings in Alzheimer's and Niemann Pick C's disease. *Pharmacopsychiatry*, **36** (Suppl 2), S120–731126.
18. Wolfe, M.S. (2012) The role of tau in neurodegenerative diseases and its potential as a therapeutic target. *Scientifica*, **2012**, 1–20.
19. Züchner, S., Wang, G., Tran-Viet, K.-N., Nance, M.A., Gaskell, P.C., Vance, J.M., Ashley-Koch, A.E. and Pericak-Vance, M.A. (2006) Mutations in the novel mitochondrial protein REEP1 cause hereditary spastic paraplegia type 31. *Am. J. Hum. Genet.*, **79**, 365–369.
20. Beetz, C., Schüle, R., Deconinck, T., Tran-Viet, K.-N., Zhu, H., Kremer, B.P.H., Frints, S.G.M., van Zelst-Stams, W.A.G., Byrne, P., Otto, S. *et al.* (2008) REEP1 mutation spectrum and genotype/phenotype correlation in hereditary spastic paraplegia type 31. *Brain J. Neurol.*, **131**, 1078–1086.
21. Hewamadduma, C., McDermott, C., Kirby, J., Grierson, A., Panayi, M., Dalton, A., Rajabally, Y. and Shaw, P. (2009) New pedigrees and novel mutation expand the phenotype of REEP1-associated hereditary spastic paraplegia (HSP). *Neurogenetics*, **10**, 105–110.
22. Park, S.H., Zhu, P.-P., Parker, R.L. and Blackstone, C. (2010) Hereditary spastic paraplegia proteins REEP1, spastin, and atlastin-1 coordinate microtubule interactions with the tubular ER network. *J. Clin. Invest.*, **120**, 1097–1110.
23. McCorquodale, D.S. 3rd, Ozomaro, U., Huang, J., Montenegro, G., Kushman, A., Citrigno, L., Price, J., Speziani, F., Pericak-Vance, M.A. and Züchner, S. (2011) Mutation screening of spastin, atlastin, and REEP1 in hereditary spastic paraplegia. *Clin. Genet.*, **79**, 523–530.
24. Beetz, C., Pieber, T.R., Hertel, N., Schabhüttl, M., Fischer, C., Trajanoski, S., Graf, E., Keiner, S., Kurth, I., Wieland, T. *et al.* (2012) Exome sequencing identifies a REEP1 mutation involved in distal hereditary motor neuropathy type V. *Am. J. Hum. Genet.*, **91**, 139–145.
25. Bernstein, E., Caudy, A.A., Hammond, S.M. and Hannon, G.J. (2001) Role for a bidentate ribonuclease in the initiation step of RNA interference. *Nature*, **409**, 363–366.
26. Dietzl, G., Chen, D., Schnorrer, F., Su, K.-C., Barinova, Y., Fellner, M., Gasser, B., Kinsey, K., Oppel, S., Scheiblauer, S. *et al.* (2007) A genome-wide transgenic RNAi library for conditional gene inactivation in Drosophila. *Nature*, **448**, 151–156.
27. Beetz, C., Koch, N., Khundadze, M., Zimmer, G., Nietzsche, S., Hertel, N., Huebner, A.-K., Mumtaz, R., Schweizer, M., Dirren, E. *et al.* (2013) A spastic paraplegia mouse model reveals REEP1-dependent ER shaping. *J. Clin. Invest.*, **123**, 4273–4282.
28. Björk, S., Hurt, C.M., Ho, V.K. and Angelotti, T. (2013) REEPs are membrane shaping adapter proteins that modulate specific g protein-coupled receptor trafficking by affecting ER cargo capacity. *PLoS ONE*, **8**, e76366.
29. Chigurupati, S., Wei, Z., Belal, C., Vandermey, M., Kyriazis, G.A., Arumugam, T.V. and Chan, S.L. (2009) The homocysteine-inducible endoplasmic reticulum stress protein counteracts calcium store depletion and induction of CCAAT enhancer-binding protein homologous protein in a neurotoxin model of parkinson disease. *J. Biol. Chem.*, **284**, 18323–18333.
30. Hetz, C. and Mollereau, B. (2014) Disturbance of endoplasmic reticulum proteostasis in neurodegenerative diseases. *Nat. Rev. Neurosci.*, **15**, 233–249.
31. Hoozemans, J.J.M., Veerhuis, R., Haastert, E.S.V., Rozemuller, J.M., Baas, F., Eikelenboom, P. and Scheper, W. (2005) The unfolded protein response is activated in Alzheimer's disease. *Acta Neuropathol. (Berl.)*, **110**, 165–172.
32. Loewen, C.A. and Feany, M.B. (2010) The unfolded protein response protects from tau neurotoxicity in vivo. *PLoS ONE*, **5**, e13084.
33. Berrigan, D., Hercus, M., Dagher, H. and Hoffmann, A.A. (1997) Comparing different measures of heat resistance in selected lines of Drosophila melanogaster. *J. Insect Physiol.*, **43**, 393–405.
34. Girardot, F., Monnier, V. and Tricoire, H. (2004) Genome wide analysis of common and specific stress responses in adult drosophila melanogaster. *BMC Genomics*, **5**, 74–90.
35. Huey, R.B., Crill, W.D., Kingsolver, J.G. and Weber, K.E. (1992) A method for rapid measurement of heat or cold resistance of small insects. *Funct. Ecol.*, **6**, 489.
36. Chan, C.-C., Scoggin, S., Wang, D., Cherry, S., Dembo, T., Greenberg, B., Jin, E.J., Kuey, C., Lopez, A., Mehta, S.Q. *et al.* (2011) Systematic discovery of Rab GTPases with synaptic functions in Drosophila. *Curr. Biol.*, **21**, 1704–1715.
37. Dricu, A., Carlberg, M., Wang, M. and Larsson, O. (1997) Inhibition of N-linked glycosylation using tunicamycin causes cell death in malignant cells: role of down-regulation of the insulin-like growth factor 1 receptor in induction of apoptosis. *Cancer Res.*, **57**, 543–548.
38. Harding, H.P., Zhang, Y. and Ron, D. (1999) Protein translation and folding are coupled by an endoplasmic-reticulum-resident kinase. *Nature*, **397**, 271–274.
39. Bertolotti, A., Zhang, Y., Hendershot, L.M., Harding, H.P. and Ron, D. (2000) Dynamic interaction of BiP and ER stress transducers in the unfolded-protein response. *Nat. Cell Biol.*, **2**, 326–332.
40. Lai, E., Teodoro, T. and Volchuk, A. (2007) Endoplasmic reticulum stress: signaling the unfolded protein response. *Physiology*, **22**, 193–201.
41. Fulga, T.A., Elson-Schwab, I., Khurana, V., Steinhilb, M.L., Spires, T.L., Hyman, B.T. and Feany, M.B. (2007) Abnormal bundling and accumulation of F-actin mediates tau-induced neuronal degeneration in vivo. *Nat. Cell Biol.*, **9**, 139–148.
42. Biernat, J., Mandelkow, E.M., Schroter, C., Lichtenberg-Kraag, B., Steiner, B., Berling, B., Meyer, H., Mercken, M., Vandermeeren, A. and Goedert, M. (1992) The switch of tau protein to an Alzheimer-like state includes the phosphorylation of two serine-proline motifs upstream of the microtubule binding region. *EMBO J.*, **11**, 1593–1597.

43. Goedert, M., Jakes, R., Crowther, R.A., Cohen, P., Vanmechelen, E., Vandermeeren, M. and Cras, P. (1994) Epitope mapping of monoclonal antibodies to the paired helical filaments of Alzheimer's disease: identification of phosphorylation sites in tau protein. *Biochem. J.*, **301**, 871–877.
44. Goedert, M., Jakes, R. and Vanmechelen, E. (1995) Monoclonal antibody AT8 recognises tau protein phosphorylated at both serine 202 and threonine 205. *Neurosci. Lett.*, **189**, 167–169.
45. Mercken, M., Vandermeeren, M., Lübke, U., Six, J., Boons, J., Van de Voorde, A., Martin, J.J. and Gheuens, J. (1992) Monoclonal antibodies with selective specificity for Alzheimer Tau are directed against phosphatase-sensitive epitopes. *Acta Neuropathol. (Berl.)*, **84**, 265–272.
46. LoPresti, P., Szuchet, S., Papasozomenos, S.C., Zinkowski, R.P. and Binder, L.I. (1995) Functional implications for the microtubule-associated protein tau: localization in oligodendrocytes. *Proc. Natl. Acad. Sci.*, **92**, 10369–10373.
47. Chen, C.-N., Chu, C.-C., Zentella, R., Pan, S.-M. and Ho, T.-H.D. (2002) AtHVA22 gene family in Arabidopsis: phylogenetic relationship, ABA and stress regulation, and tissue-specific expression. *Plant Mol. Biol.*, **49**, 633–644.
48. Guo, W.-J., Ho, T.-H. and David Ho, T.-H. (2008) An abscisic acid-induced protein, HVA22, inhibits gibberellin-mediated programmed cell death in cereal aleurone cells. *Plant Physiol.*, **147**, 1710–1722.
49. Calero, M., Whittaker, G.R. and Collins, R.N. (2001) Yop1p, the yeast homolog of the polyposis locus protein 1, interacts with Yip1p and negatively regulates cell growth. *J. Biol. Chem.*, **276**, 12100–12112.
50. Schaeffer, V., Lavenir, I., Ozcelik, S., Tolnay, M., Winkler, D.T. and Goedert, M. (2012) Stimulation of autophagy reduces neurodegeneration in a mouse model of human tauopathy. *Brain J. Neurol.*, **135**, 2169–2177.
51. Chesser, A.S., Pritchard, S.M. and Johnson, G.V.W. (2013) Tau clearance mechanisms and their possible role in the pathogenesis of Alzheimer disease. *Front. Neurol.*, **4**, 122–134.
52. Miura, S., Shibata, H., Kida, H., Noda, K., Toyama, T., Iwasaki, N., Iwaki, A., Ayabe, M., Aizawa, H., Taniwaki, T. *et al.* (2011) Partial SPAST and DPY30 deletions in a Japanese spastic paraplegia type 4 family. *Neurogenetics*, **12**, 25–31.
53. Denton, K.R., Lei, L., Grenier, J., Rodionov, V., Blackstone, C. and Li, X.-J. (2014) Loss of spastin function results in disease-specific axonal defects in human pluripotent stem cell-based models of hereditary spastic paraplegia. *Stem Cells*, **32**, 414–423.
54. Bland, M.L., Lee, R.J., Magallanes, J.M., Foskett, J.K. and Birnbaum, M.J. (2010) AMPK supports growth in Drosophila by regulating muscle activity and nutrient uptake in the gut. *Dev. Biol.*, **344**, 293–303.
55. Li, W.-Z., Li, S.-L., Zheng, H.Y., Zhang, S.-P. and Xue, L. (2012) A broad expression profile of the GMR-GAL4 driver in Drosophila melanogaster. *Genet. Mol. Res.*, **11**, 1997–2002.
56. Wu, J.S. and Luo, L. (2006) A protocol for dissecting Drosophila melanogaster brains for live imaging or immunostaining. *Nat. Protoc.*, **1**, 2110–2115.